

# AM<sup>V</sup>M<sup>III</sup>(PO<sub>4</sub>)<sub>3</sub>: New Mixed-Metal Phosphates Having NASICON and Related Structures<sup>‡</sup>

K. Kasthuri Rangan and J. Gopalakrishnan\*

Solid State and Structural Chemistry Unit,  
Indian Institute of Science, Bangalore 560 012, India

Received September 20, 1994

## Introduction

NaZr<sub>2</sub>(PO<sub>4</sub>)<sub>3</sub><sup>1</sup> is the prototype of an extensive family of solid materials that are referred to as NASICONs or NZPs in the literature.<sup>2,3</sup> The widespread interest in this family stems from the seminal discovery<sup>4</sup> of fast sodium ion transport in the silicophosphate series Na<sub>1+x</sub>Zr<sub>2</sub>P<sub>3-x</sub>Si<sub>x</sub>O<sub>12</sub> (NASICON), which possesses the NaZr<sub>2</sub>(PO<sub>4</sub>)<sub>3</sub> (NZP) framework.<sup>1,5</sup> The Zr<sub>2</sub>(XO<sub>4</sub>)<sub>3</sub> framework, consisting of ZrO<sub>6</sub> octahedra and XO<sub>4</sub> (X = P, Si) tetrahedra linked by corners, provides an interconnected interstitial space where the mobile sodium or other cations are located. Besides fast-ion conductivity, members of this family have been explored for other properties as well, such as immobilization of radioactive nuclides,<sup>6</sup> low thermal expansion,<sup>7</sup> and ion-exchange<sup>8</sup> and redox insertion/extraction reactions.<sup>9</sup> The unique M<sub>2</sub>(XO<sub>4</sub>)<sub>3</sub> framework of the NASICON/NZP structure enables a variety of chemical substitutions to be made both at the framework and at the interstitial sites enclosed by the framework. A recent review by Alamo<sup>3</sup> lists all the possible NASICON derivatives obtained so far by various chemical substitutions. Here, we report a new chemical substitution in the NZP structure, viz., 2Zr<sup>IV</sup> → M<sup>V</sup> + M<sup>III</sup>, where M<sup>V</sup> = Nb or Ta and M<sup>III</sup> = Ti, V, Cr, Fe, or Al, that has enabled us to synthesize several members of the general formula AM<sup>V</sup>M<sup>III</sup>(PO<sub>4</sub>)<sub>3</sub>. To our knowledge, NaNbTi(PO<sub>4</sub>)<sub>3</sub> is the only member of this series that has been previously reported<sup>10</sup> as a part of Na<sub>x</sub>NbTi(PO<sub>4</sub>)<sub>3</sub>. Besides enlarging the NZP structure field to include several M<sup>V</sup>–M<sup>III</sup> combinations at octahedral sites in the framework, the present work also shows the possibility of oxidative deintercalation of sodium from NaNbTi(PO<sub>4</sub>)<sub>3</sub> and NaNbV(PO<sub>4</sub>)<sub>3</sub> leaving the NZP framework intact.

## Experimental Section

NaM<sup>V</sup>M<sup>III</sup>(PO<sub>4</sub>)<sub>3</sub> phosphates for M<sup>V</sup> = Nb or Ta and M<sup>III</sup> = Ti or V were prepared by reacting preheated stoichiometric mixtures of Na<sub>2</sub>CO<sub>3</sub>, M<sup>V</sup><sub>2</sub>O<sub>5</sub>, TiO<sub>2</sub>/V<sub>2</sub>O<sub>5</sub>, and (NH<sub>4</sub>)<sub>2</sub>HPO<sub>4</sub> at 950 °C for 3 days in a flowing hydrogen atmosphere (~10 mL/min). Similar phosphates for M<sup>III</sup> = Cr, Fe, or Al were prepared by direct solid state reactions in air employing Cr<sub>2</sub>O<sub>3</sub>, Fe<sub>2</sub>O<sub>3</sub>, or Al<sub>2</sub>O<sub>3</sub>. The corresponding lithium compounds were prepared by the same method using Li<sub>2</sub>CO<sub>3</sub> at 800 °C for 24 h. Deintercalation of sodium from NaNbTi(PO<sub>4</sub>)<sub>3</sub> and NaNbV(PO<sub>4</sub>)<sub>3</sub> (M = Nb, Ta) was carried out<sup>9c</sup> by passing chlorine through a suspension of ~2 g of the powder in 50 mL of CHCl<sub>3</sub>. Oxidation

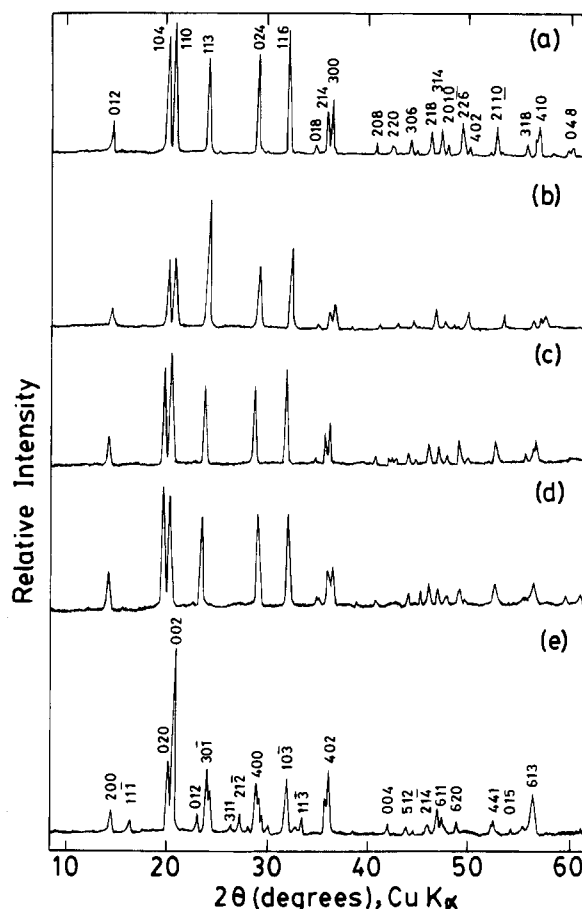


Figure 1. X-ray powder diffraction patterns of (a) NaTaCr(PO<sub>4</sub>)<sub>3</sub>, (b) NaNbAl(PO<sub>4</sub>)<sub>3</sub>, (c) NaTaV(PO<sub>4</sub>)<sub>3</sub>, (d) TaV(PO<sub>4</sub>)<sub>3</sub>, and (e) LiNbV(PO<sub>4</sub>)<sub>3</sub>.

states of titanium and vanadium in the compounds were determined by redox potentiometric titration using Ce(IV) as oxidizing agent.

The new phosphates were characterized by powder X-ray diffraction (XRD) (JEOL JDX-8P X-ray diffractometer, Cu K $\alpha$  radiation), infrared absorption spectroscopy (Bio-Rad, SKC-3200 FTIR spectrometer), and <sup>27</sup>Al NMR spectroscopy (Bruker MSL-300 spectrometer operating at 78.21 MHz). Lattice parameters were derived from least-squares refinement of the powder X-ray diffraction data using PROSZKI program<sup>11</sup> that includes LAZY PULVERIX.

## Results and Discussion

The basic structural unit of the NZP framework is [Zr<sub>2</sub>P<sub>3</sub>O<sub>12</sub>]<sup>-</sup>, which consists of two ZrO<sub>6</sub> octahedra joined by three PO<sub>4</sub> tetrahedra.<sup>1</sup> This unit repeats along the *c* direction forming columns which are in turn connected by PO<sub>4</sub> tetrahedra to form the framework. A number of substitutions at the zirconium site of NZP have been investigated, giving rise to a variety of NASICON derivatives.<sup>3</sup> A straightforward substitution would be 2Zr<sup>IV</sup> → M<sup>V</sup> + M<sup>III</sup>, which has not been explored in the literature. Accordingly, we investigated the formation of NZP-type phases of the general formula AM<sup>V</sup>M<sup>III</sup>(PO<sub>4</sub>)<sub>3</sub>, for M<sup>V</sup> = Nb or Ta with a number of trivalent metals. We could readily prepare such phases for M<sup>III</sup> = Cr, Fe, or Al by direct solid state reactions of the constituents in air, while the syntheses of the corresponding M<sup>III</sup> = Ti or V phases required hydrogen reduction of preheated stoichiometric mixtures containing TiO<sub>2</sub> or V<sub>2</sub>O<sub>5</sub>. While we could obtain NZP-type phases for A = Na or Li, our attempts to prepare similar phases for A = K resulted in multiphase mixtures containing both Langbeinite and NASICON/NZP-type structures.

\* Author to whom correspondence should be addressed.

<sup>‡</sup> Contribution No. 1074 from the Solid State and Structural Chemistry Unit.

- (1) Hagman, L.; Kierkegaard, P. *Acta Chem. Scand.* **1968**, *22*, 1822.
- (2) Kanazawa, T. *Inorganic Phosphate Materials*; Kodansha: Tokyo, 1989; Chapter 7.
- (3) Alamo, J. *Solid State Ionics* **1993**, *63–65*, 547.
- (4) Goodenough, J. B.; Hong, H. Y.-P.; Kafalas, J. A. *Mater. Res. Bull.* **1976**, *11*, 203.
- (5) Hong, H. Y.-P. *Mater. Res. Bull.* **1976**, *11*, 173.
- (6) Roy, R.; Vance, E. R.; Alamo, J. *Mater. Res. Bull.* **1982**, *17*, 585.
- (7) Alamo, J.; Roy, R. *J. Mater. Sci.* **1986**, *21*, 444.
- (8) Hirose, N.; Kuwano, J. *J. Mater. Chem.* **1994**, *4*, 9.
- (9) (a) Delmas, C.; Cherkaoui, F.; Nadiri, A.; Hagenmuller, P. *Mater. Res. Bull.* **1987**, *22*, 631. (b) Delmas, C.; Nadiri, A.; Soubeyroux, J. L. *Solid State Ionics* **1988**, *28–30*, 419. (c) Gopalakrishnan, J.; Kasthuri Rangan, K. *Chem. Mater.* **1992**, *4*, 745.

**Table 1.** Composition, Color, and Lattice Parameters of  $AM^VM^{III}(PO_4)_3$  Phosphates and their Derivatives

| composition                           | color          | reducing power |                       | lattice parameters (Å) |           |
|---------------------------------------|----------------|----------------|-----------------------|------------------------|-----------|
|                                       |                | found          | expected <sup>a</sup> | <i>a</i>               | <i>c</i>  |
| NaNbTi(PO <sub>4</sub> ) <sub>3</sub> | dark blue      | 0.97           | 1.00                  | 8.630(4)               | 22.052(5) |
| NaNbV(PO <sub>4</sub> ) <sub>3</sub>  | brownish green | 2.01           | 2.00                  | 8.565(6)               | 22.078(8) |
| NaNbCr(PO <sub>4</sub> ) <sub>3</sub> | green          |                |                       | 8.515(6)               | 22.023(7) |
| NaNbFe(PO <sub>4</sub> ) <sub>3</sub> | pale pink      |                |                       | 8.571(5)               | 22.102(9) |
| NaNbAl(PO <sub>4</sub> ) <sub>3</sub> | white          |                |                       | 8.476(8)               | 21.810(5) |
| NaTaV(PO <sub>4</sub> ) <sub>3</sub>  | green          | 2.00           | 2.00                  | 8.587(3)               | 22.089(6) |
| NaTaCr(PO <sub>4</sub> ) <sub>3</sub> | green          |                |                       | 8.546(4)               | 22.065(9) |
| NaTaFe(PO <sub>4</sub> ) <sub>3</sub> | pale pink      |                |                       | 8.580(3)               | 22.149(6) |
| NaTaAl(PO <sub>4</sub> ) <sub>3</sub> | white          |                |                       | 8.471(4)               | 21.928(6) |
| LiNbV(PO <sub>4</sub> ) <sub>3</sub>  | green          | 1.99           | 2.00                  | <i>b</i>               |           |
| LiNbFe(PO <sub>4</sub> ) <sub>3</sub> | pale pink      |                |                       | 8.589(6)               | 21.654(8) |
| LiTaV(PO <sub>4</sub> ) <sub>3</sub>  | green          | 2.00           | 2.00                  | <i>c</i>               |           |
| LiTaCr(PO <sub>4</sub> ) <sub>3</sub> | green          |                |                       | 8.535(6)               | 21.551(8) |
| LiTaFe(PO <sub>4</sub> ) <sub>3</sub> | pale pink      |                |                       | 8.608(6)               | 21.753(6) |
| LiTaAl(PO <sub>4</sub> ) <sub>3</sub> | white          |                |                       | 8.510(5)               | 21.230(4) |
| TaV(PO <sub>4</sub> ) <sub>3</sub>    | green          | 1.02           | 1.00                  | 8.514(5)               | 21.949(8) |
| NbTi(PO <sub>4</sub> ) <sub>3</sub>   | white          |                |                       | 8.552(2)               | 21.945(6) |

<sup>a</sup> Corresponds to the number of electrons per formula unit required for the oxidation of titanium and vanadium. <sup>b</sup> Monoclinic:  $a = 12.282(9)$ ,  $b = 8.764(8)$ ,  $c = 8.590(5)$  Å;  $\beta = 90.90(8)^\circ$ . <sup>c</sup> Monoclinic:  $a = 12.27(1)$ ,  $b = 8.773(8)$ ,  $c = 8.590(8)$  Å;  $\beta = 90.63(8)^\circ$ .

**Table 2.** X-ray Powder Diffraction Data for NaTaCr(PO<sub>4</sub>)<sub>3</sub>

| <i>hkl</i>     | $d_{obs}$ (Å) | $d_{cal}$ (Å)      | $I_{obs}$ | $I_{cal}^a$ |
|----------------|---------------|--------------------|-----------|-------------|
| 012            | 6.135         | 6.146              | 24        | 23          |
| 104            | 4.412         | 4.423              | 86        | 84          |
| 110            | 4.275         | 4.273              | 100       | 100         |
| 113            | 3.686         | 3.695              | 67        | 64          |
| 024            | 3.070         | 3.073              | 72        | 52          |
| 116 }<br>211 } | 2.788         | 2.787 }<br>2.775 } | 80        | 68 }<br>8 } |
| 018            | 2.578         | 2.584              | 9         | 7           |
| 214            | 2.488         | 2.495              | 31        | 25          |
| 300            | 2.462         | 2.467              | 40        | 38          |
| 208            | 2.206         | 2.211              | 9         | 7           |
| 220            | 2.132         | 2.137              | 7         | 6           |
| 1,0,10         | 2.108         | 2.115              | 4         | 4           |
| 217            | 2.087         | 2.092              | 1         | 1           |
| 306            | 2.045         | 2.049              | 10        | 8           |
| 312            | 2.014         | 2.018              | 1         | 1           |
| 218            | 1.961         | 1.961              | 23        | 20          |
| 314            | 1.922         | 1.923              | 18        | 13          |
| 2,0,10         | 1.895         | 1.895              | 9         | 7           |
| 226            | 1.843         | 1.847              | 27        | 22          |
| 402            | 1.822         | 1.825              | 5         | 3           |
| 2,1,10         | 1.731         | 1.732              | 23        | 19          |
| 137            | 1.719         | 1.720              | 6         | 3           |
| 318            | 1.645         | 1.647              | 13        | 10          |
| 324            | 1.621         | 1.623              | 15        | 12          |
| 410            | 1.613         | 1.615              | 29        | 23          |
| 048            | 1.535         | 1.537              | 7         | 5           |

<sup>a</sup> Calculated by the LAZY PULVERIX program using the position parameters of NaZr<sub>2</sub>(PO<sub>4</sub>)<sub>3</sub>.<sup>1</sup>

We give the XRD patterns of the representative members of  $AM^VM^{III}(PO_4)_3$  in Figure 1; in Table 1, we list the unit cell parameters together with other characteristics of all the phosphates synthesized. We see that while most of the phases synthesized crystallize in the rhombohedral ( $R\bar{3}c$ ) NZP structure,<sup>1</sup> LiMV(PO<sub>4</sub>)<sub>3</sub> ( $M = Nb, Ta$ ) crystallize in a monoclinic structure probably related to Ni<sub>0.5</sub>Zr<sub>2</sub>(PO<sub>4</sub>)<sub>3</sub>.<sup>12</sup> In Tables 2 and 3, we give indexed powder X-ray diffraction data for representative members of both structure types. We have also calculated the intensities of *hkl* reflections for the rhombohedral phases, using the position parameters<sup>1</sup> of NaZr<sub>2</sub>(PO<sub>4</sub>)<sub>3</sub> and assuming a

**Table 3.** X-ray Powder Diffraction Data for LiNbV(PO<sub>4</sub>)<sub>3</sub>

| <i>hkl</i> | $d_{obs}$ (Å) | $d_{cal}$ (Å) | $I_{obs}$ |
|------------|---------------|---------------|-----------|
| 200        | 6.150         | 6.140         | 14        |
| 111        | 5.471         | 5.513         | 8         |
| 020        | 4.439         | 4.382         | 39        |
| 002        | 4.301         | 4.294         | 100       |
| 012        | 3.858         | 3.856         | 11        |
| 301        | 3.708         | 3.718         | 36        |
| 301        | 3.670         | 3.673         | 23        |
| 311        | 3.363         | 3.387         | 5         |
| 212        | 3.267         | 3.286         | 11        |
| 400        | 3.079         | 3.070         | 31        |
| 022        | 3.053         | 3.067         | 22        |
| 320        | 3.023         | 2.991         | 10        |
| 122        | 2.959         | 2.968         | 5         |
| 103        | 2.797         | 2.797         | 31        |
| 411        | 2.730         | 2.733         | 4         |
| 013        | 2.714         | 2.721         | 4         |
| 113        | 2.675         | 2.665         | 9         |
| 203        | 2.501         | 2.501         | 18        |
| 402        | 2.481         | 2.479         | 35        |
| 040        | 2.212         | 2.191         | 3         |
| 004        | 2.151         | 2.147         | 6         |
| 512        | 2.060         | 2.058         | 5         |
| 204        | 2.029         | 2.036         | 2         |
| 214        | 1.971         | 1.984         | 6         |
| 611        | 1.931         | 1.935         | 14        |
| 522        | 1.910         | 1.907         | 9         |
| 620        | 1.855         | 1.855         | 6         |
| 503        | 1.848         | 1.849         | 5         |
| 441        | 1.743         | 1.743         | 5         |
| 324        | 1.737         | 1.735         | 8         |
| 015        | 1.685         | 1.685         | 3         |
| 251        | 1.653         | 1.653         | 5         |
| 613        | 1.623         | 1.624         | 23        |

random distribution of  $M^V$  and  $M^{III}$  atoms at the 12(c) site. We see that the agreement between the observed and calculated intensities is quite good (Table 2), suggesting that the NZP model is most likely for the rhombohedral  $AM^VM^{III}(PO_4)_3$  phases.

The powder XRD patterns (Figure 1 and Table 3) of monoclinic LiNbV(PO<sub>4</sub>)<sub>3</sub> and LiTaV(PO<sub>4</sub>)<sub>3</sub> show a strong resemblance to that of Ni<sub>0.5</sub>Zr<sub>2</sub>(PO<sub>4</sub>)<sub>3</sub>.<sup>12</sup> Accordingly, we could index the patterns of these phases on monoclinic cells with lattice parameters  $a = 12.282(9)$  Å,  $b = 8.764(4)$  Å,  $c = 8.590(5)$  Å,  $\beta = 90.90(8)^\circ$  for LiNbV(PO<sub>4</sub>)<sub>3</sub> and  $a = 12.27(1)$  Å,  $b = 8.773(8)$  Å,  $c = 8.590(8)$  Å,  $\beta = 90.63(8)^\circ$  for LiTaV(PO<sub>4</sub>)<sub>3</sub>. The monoclinic ( $P2_1/n$ ) structure of Ni<sub>0.5</sub>Zr<sub>2</sub>(PO<sub>4</sub>)<sub>3</sub> has been shown to be related to the structure of Sc<sub>2</sub>(WO<sub>4</sub>)<sub>3</sub>.<sup>12</sup> The Sc<sub>2</sub>(WO<sub>4</sub>)<sub>3</sub> structure, which appears to be competitive with the NZP/NASICON structure, is adopted by  $A_xM_2(XO_4)_3$  compounds for small A cations such as Li, Mg, Ni, or Cu. It is interesting that, among the various  $LiM^VM^{III}(PO_4)_3$  phases synthesized here, only the  $M^{III} = V$  compounds crystallize with this structure.

In Figure 2, we have plotted the hexagonal *a* and *c* parameters of rhombohedral  $NaNb^VM^{III}(PO_4)_3$  as a function of the average ionic radius<sup>13</sup> of the octahedral site cations. For purposes of comparison, we have also included the data for the corresponding Zr<sup>IV</sup>, Ti<sup>IV</sup>, and Ge<sup>IV</sup> phosphates.<sup>1</sup> We see that the variation of *a* and *c* with the average ionic radius is almost linear for all compositions excepting the Ge<sup>IV</sup> phosphate. The anomalous behavior of the Ge<sup>IV</sup> phase is likely related to the fact that it adopts a different space group ( $R\bar{3}$ ).<sup>14</sup> Among the new phosphates reported in this paper, those containing Al<sup>III</sup> deserve

(11) Lasocha, W.; Lewinski, K. *J. Appl. Crystallogr.* **1994**, *27*, 437.(12) Jouanneaux, A.; Verbaere, A.; Piffard, Y.; Fitch, A.-N.; Kinoshita, M. *Eur. J. Solid State Inorg. Chem.* **1991**, *28*, 683.(13) Shannon, R. D. *Acta Crystallogr.* **1976**, *A32*, 751.(10) Tillement, O.; Couturier, J. C.; Angenault, J.; Quaron, M. *Solid State Ionics* **1991**, *48*, 249.

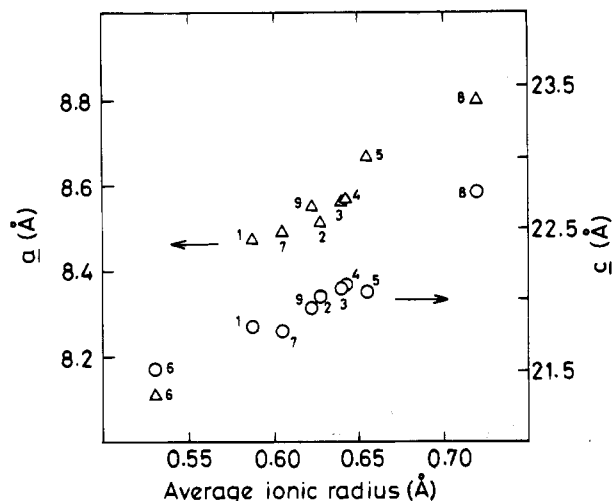


**Figure 2.** Variation of hexagonal  $a$  and  $c$  parameters of  $\text{NaNbM}^{\text{III}}(\text{PO}_4)_3$  with the average ionic radii of Nb and  $\text{M}^{\text{III}}$ . (1)  $\text{M}^{\text{III}} = \text{Al}$ ; (2)  $\text{M}^{\text{III}} = \text{Cr}$ ; (3)  $\text{M}^{\text{III}} = \text{V}$ ; (4)  $\text{M}^{\text{III}} = \text{Fe}$ ; (5)  $\text{M}^{\text{III}} = \text{Ti}$ ; (6), (7), and (8) denote corresponding data points for the  $\text{Ge}^{\text{IV}}$ ,  $\text{Ti}^{\text{IV}}$ , and  $\text{Zr}^{\text{IV}}$  phosphates, respectively; (9) denotes the data point for  $\text{NbTi}^{\text{IV}}(\text{PO}_4)_3$ .

**Table 4.** X-ray Powder Diffraction Data for  $\text{NaNbAl}(\text{PO}_4)_3$

| $hkl$          | $d_{\text{obs}}$ (Å) | $d_{\text{cal}}$ (Å) | $I_{\text{obs}}$ | $I_{\text{cal}}^a$ |
|----------------|----------------------|----------------------|------------------|--------------------|
| 012            | 6.088                | 6.089                | 20               | 16                 |
| 104            | 4.375                | 4.377                | 40               | 36                 |
| 110            | 4.240                | 4.238                | 54               | 47                 |
| 113            | 3.663                | 3.661                | 100              | 100                |
| 024            | 3.043                | 3.045                | 40               | 30                 |
| 116 }<br>211 } | 2.759                | 2.759 }<br>2.752 }   | 64               | 51<br>14           |
| 018            | 2.550                | 2.556                | 2                | 2                  |
| 214            | 2.471                | 2.473                | 9                | 7                  |
| 300            | 2.445                | 2.447                | 18               | 23                 |
| 208            | 2.191                | 2.189                | 4                | 4                  |
| 119            | 2.106                | 2.104                | 4                | 5                  |
| 306            | 2.032                | 2.030                | 6                | 3                  |
| 218            | 1.945                | 1.945                | 16               | 16                 |
| 314            | 1.910                | 1.907                | 6                | 5                  |
| 2,0,10         | 1.873                | 1.875                | 3                | 3                  |
| 226            | 1.831                | 1.831                | 14               | 18                 |
| 402            | 1.811                | 1.810                | 3                | 3                  |
| 2,1,10         | 1.713                | 1.715                | 11               | 11                 |
| 137            | 1.708                | 1.704                | 5                | 5                  |
| 318            | 1.630                | 1.631                | 9                | 8                  |
| 324            | 1.610                | 1.609                | 6                | 7                  |
| 410            | 1.603                | 1.602                | 12               | 16                 |

<sup>a</sup> Calculated by the LAZY PULVERIX program using the position parameters of  $\text{NaNbAl}(\text{PO}_4)_3$ .<sup>1</sup>

a special mention, because it has been reported<sup>15</sup> that  $\text{Al}^{\text{III}}$  does not substitute for  $\text{Zr}^{\text{IV}}$  in the NZZP structure. Our calculations of the powder XRD intensities of the  $\text{Al}^{\text{III}}$ -containing phosphates assuming the NZZP structure model give a good agreement with the observed intensities (Table 4). In addition, we recorded the solid state  $^{27}\text{Al}$  NMR spectra of  $\text{NaNbAl}(\text{PO}_4)_3$  and  $\text{NaTaAl}(\text{PO}_4)_3$  (Figure 3). The  $^{27}\text{Al}$  resonances occurring at  $-15$  and  $-19$  ppm relative to  $[\text{Al}(\text{H}_2\text{O})_6]^{3+}$  show that  $\text{Al}^{\text{III}}$  indeed occurs at the octahedral sites,<sup>16</sup> as expected for the NZZP structure model. It is likely that  $\text{Al}^{\text{III}}$  does not substitute for  $\text{Zr}^{\text{IV}}$  in  $\text{NaNbZr}(\text{PO}_4)_3$ , but it does substitute at the octahedral site of the NZZP structure, when it is coupled with pentavalent cations ( $\text{Nb}^{\text{V}}$  or  $\text{Ta}^{\text{V}}$ ) as in  $\text{NaNbAl}(\text{PO}_4)_3$  and  $\text{NaTaAl}(\text{PO}_4)_3$  reported here.

(14) Carrasco, M. P.; Guillem, M. C.; Alamo, J. *Mater. Res. Bull.* **1993**, *28*, 793.

(15) Saito, Y.; Ado, K.; Asai, T.; Kageyama, H.; Nakamura, O. *Solid State Ionics* **1992**, *58*, 327.

(16) Dupree, R.; Lewis, M. H.; Smith, M. E. *J. Appl. Crystallogr.* **1988**, *21*, 109.

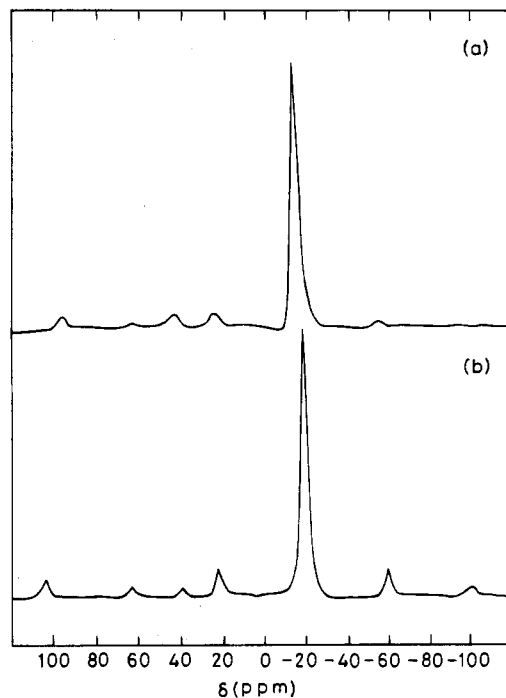


**Figure 3.**  $^{27}\text{Al}$  NMR spectra of (a)  $\text{NaNbAl}(\text{PO}_4)_3$  and (b)  $\text{NaTaAl}(\text{PO}_4)_3$ .

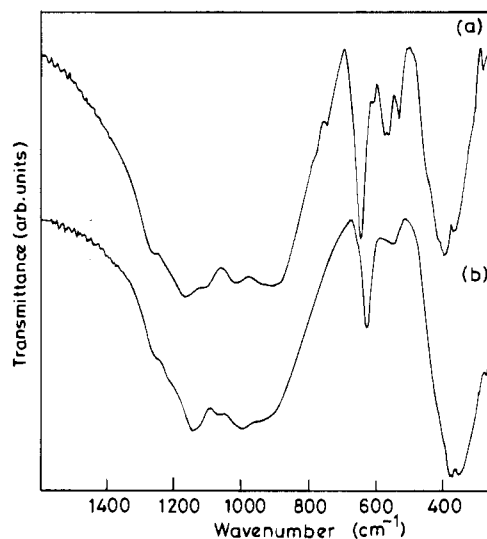


**Figure 4.** Infrared absorption spectra of (a)  $\text{NaTaV}(\text{PO}_4)_3$  and (b)  $\text{TaV}(\text{PO}_4)_3$ .

We recently showed that sodium could be deintercalated from NASICON-type  $\text{Na}_3\text{V}_2(\text{PO}_4)_3$  by reaction with chlorine in nonaqueous solvents.<sup>9c</sup> We have investigated the possibility of similar deintercalation of sodium in  $\text{NaM}^{\text{V}}\text{Ti}(\text{PO}_4)_3$  and  $\text{NaM}^{\text{V}}(\text{PO}_4)_3$ . Deintercalation readily occurs, yielding  $\text{TaV}^{\text{IV}}(\text{PO}_4)_3$  and  $\text{NbTi}^{\text{IV}}(\text{PO}_4)_3$ . Of the two,  $\text{NbTi}^{\text{IV}}(\text{PO}_4)_3$  has already been reported.<sup>17</sup> The XRD patterns (Figure 1) of these materials reveal that the NASICON framework is retained, albeit with a slight decrease in the  $a$  and  $c$  parameters ( $a = 8.514(5)$ ,  $c = 21.949(8)$  Å for  $\text{TaV}^{\text{IV}}(\text{PO}_4)_3$ ). The infrared spectra of  $\text{NaTaV}(\text{PO}_4)_3$  and its deintercalation product are shown in Figure 4. Both compounds show characteristic  $\text{PO}_4$  vibrations of the NZZP framework.<sup>18</sup> ( $1270\text{--}1070$   $\text{cm}^{-1}$ ,  $\nu_3(\text{PO}_4)$ ;  $1010\text{--}900$   $\text{cm}^{-1}$ ,

(17) Masse, R.; Durif, A.; Guitel, J. C.; Tordjman, I. *Bull. Soc. Fr. Mineral. Cristallogr.* **1972**, *95*, 47.

(18) (a) Barj, M.; Lucazeau, G.; Delmas, C. *J. Solid State Chem.* **1992**, *100*, 141. (b) Mbandza, A.; Bordes, E.; Courtine, P. *Mater. Res. Bull.* **1985**, *20*, 251.

$\nu_1(\text{PO}_4)$ ; 670–640  $\text{cm}^{-1}$ ,  $\nu_4(\text{PO}_4)$ ; 400–360  $\text{cm}^{-1}$ ,  $\nu_2(\text{PO}_4)$ ). A weak band at 530  $\text{cm}^{-1}$  in  $\text{NaTaV}(\text{PO}_4)_3$ , which is likely associated with  $\text{V}^{\text{III}}\text{O}_6$  octahedra, is shifted to 570  $\text{cm}^{-1}$  in the deintercalation product, consistent with the oxidation of  $\text{V}^{\text{III}}$  to  $\text{V}^{\text{IV}}$  on deintercalation.

**Acknowledgment.** We thank Professor C. N. R. Rao for valuable encouragement. Our thanks are also expressed to Mr.

P. T. Wilson, Sophisticated Instruments Facility of this institute, for recording the  $^{27}\text{Al}$  NMR spectra. We thank the Department of Science and Technology, Government of India, for financial support, and K.K.R. thanks the University Grants Commission for a fellowship.

IC9411007

## Additions and Corrections

1994, Volume 33

**Enrique Colacio,\* Jose M. Dominguez-Vera, Albert Escuer,\* Raikko Kivekäs, and Antonio Romerosa: Heterodinuclear Copper(II)–Nickel(II) Complexes with Unusual Asymmetrical Bridges from a New and Versatile Dioxime Multidentate Ligand. Magneto–Structural Study.**

Page 3920. In Table 6, some of the bond angles involving the Ni(II) atom were incorrectly reported. Corrected data are as follows:

|                 |          |                 |          |
|-----------------|----------|-----------------|----------|
| O(14)–Ni–O(15A) | 97.2(6)  | O(14)–Ni–N(15)  | 73.1(2)  |
| O(14)–Ni–N(18)  | 170.4(2) | O(14)–Ni–N(29)  | 97.9(2)  |
| O(14)–Ni–N(25)  | 87.3(2)  | O(14)–Ni–N(22)  | 88.1(2)  |
| O(15A)–Ni–N(18) | 73.6(6)  | O(15A)–Ni–N(29) | 87.0(7)  |
| O(15A)–Ni–N(25) | 174.8(6) | O(15A)–Ni–N(22) | 98.2(6)  |
| N(15)–Ni–N(18)  | 97.7(2)  | N(15)–Ni–N(29)  | 88.0(3)  |
| N(15)–Ni–N(25)  | 159.8(2) | N(15)–Ni–N(22)  | 99.6(3)  |
| N(18)–Ni–N(29)  | 84.3(2)  | N(18)–Ni–N(25)  | 102.0(2) |
| N(18)–Ni–N(22)  | 90.7(2)  | N(22)–Ni–N(25)  | 84.5(2)  |
| N(22)–Ni–N(29)  | 171.5(2) | N(25)–Ni–N(29)  | 89.7(2)  |

IC9419426